15

Climate Change in the Upper Atmosphere

Ingrid Cnossen
High Altitude Observatory, National Center for Atmospheric Research
USA

1. Introduction

Studies of climate change traditionally focus on long-term changes taking place in the troposphere. This is understandable, as this is the part of the atmosphere that most directly affects life on the surface. However, long-term trends higher in the atmosphere can have important consequences as well. The middle and upper atmosphere consist of the stratosphere (~15-50 km), the mesosphere (~50-90 km), the thermosphere (~90-800 km), and the embedded ionosphere, the ionized part of the upper atmosphere (see figure 1).

Many satellites operate within the thermosphere. Since the drag exerted upon them is proportional to the ambient atmospheric density, long-term changes in the density in the thermosphere can affect their trajectories and orbital lifetimes. Also, long-term trends in the ionosphere can affect radio wave propagation, and therefore the performance of the Global Positioning System (GPS) and other space-based navigation and communication systems that rely on radio waves (Laštovička et al., 2006a). In addition to these in-situ effects, there is evidence that perturbations in the upper atmosphere may propagate downward (e.g. Haynes et al., 1991), and that the state of the middle and upper atmosphere has an influence on the troposphere (e.g. Baldwin & Dunkerton, 2001; Sassi et al., 2010). There is thus a possibility that long-term trends in the upper atmosphere could play a role in tropospheric climate too. For these reasons it is important to gain a good understanding of the processes that cause long-term trends in this part of the atmosphere.

As in the lower atmosphere, the increase in carbon-dioxide concentration is thought to be one of the main causes for climatic changes in the upper atmosphere (Laštovička et al., 2006a). However, it has become clear in recent years that several other mechanisms for long-term change must be considered as well (e.g. Qian et al. 2011). These include changes in ozone, methane and water vapour concentration, the secular variation of the Earth's magnetic field, and long-term changes in solar and geomagnetic activity. Also climate change in the lower atmosphere could have an effect.

The aim of this chapter is to review our current knowledge of the processes mentioned above and their role in causing climate change in the upper atmosphere. A brief overview of observed trends in several variables is given first (section 2), followed by a discussion of the possible responsible mechanisms (sections 3-6). Estimates of trends caused by each of the mechanisms as determined from model simulations are compared to observed trends where possible.

2. Observed long-term trends in the upper atmosphere

2.1 Introduction

When talking about climate change, we generally are referring to quasi-linear changes or "trends" that occur over a period of ~30 years or more (by the definition of the World Meteorological Organization). In practice, climate change is not necessarily linear, and trends can (and eventually will) change over time. However, for the purposes of this chapter we will assume that trends that have been observed over the last 50-60 years, or subsets of that time frame, can be meaningfully described in terms of a linear change per decade.

To measure trends, we need high quality, long-term datasets, which are much sparser in the upper atmosphere than they are in the troposphere. In addition, the upper atmosphere is strongly influenced by the 11-year solar cycle, as well as fluctuations in geomagnetic activity (see section 5). This shorter-term variability must be corrected for to be able to detect a long-term trend. Various studies have shown that this is a non-trivial task, as different methodologies may yield different results (Laštovička et al., 2006b), and residual solar signals can remain, especially if the dataset is not sufficiently long (Clilverd et al., 2003).

Trends in the height of the peak electron density of the ionospheric F_2 layer, h_mF_2 (see figure 1), suffer from an additional complication when ionosonde data are used. In that case h_mF_2 is not directly measured, but calculated from the $M(3000)F_2$ parameter, which is a transmission factor related to the highest frequency that can be propagated between two sites 3000 km apart by ionospheric propagation alone. There are different empirical formulas to calculate h_mF_2 from $M(3000)F_2$, and unfortunately these can result in different trends from the same dataset, sometimes even with a different sign (Ulich, 2000; Jarvis et al., 2002). When incoherent scatter data are used, h_mF_2 can be directly measured, but the data record is much shorter, and far fewer sites are available.

Despite these difficulties, considerable progress has been made in building a global picture of long-term trends in the upper atmosphere. In this chapter we focus on a few selected variables for which both observational and theoretical trend estimates are available, so that the two can be directly compared. These are temperature, density, h_mF_2, and the critical frequency of the F_2 layer, f_oF_2, which is directly related to the peak electron density N_mF_2 as:

$$N_mF_2 = 1.24 \times 10^{10} (f_oF_2)^2 \quad (1)$$

where N_mF_2 is in m^{-3} and f_oF_2 is in MHz.

2.2 Temperature

Figure 1 gives a schematic overview of the observed trends in the temperature and the electron density profile, and also labels the various regions of the atmosphere. Trends in temperature have been determined from a large number of studies and a variety of measurement techniques (e.g. rocketsonde, lidar, radar, satellite data). Trends in the upper atmosphere are mostly negative, except in the mesopause/lower thermosphere region.

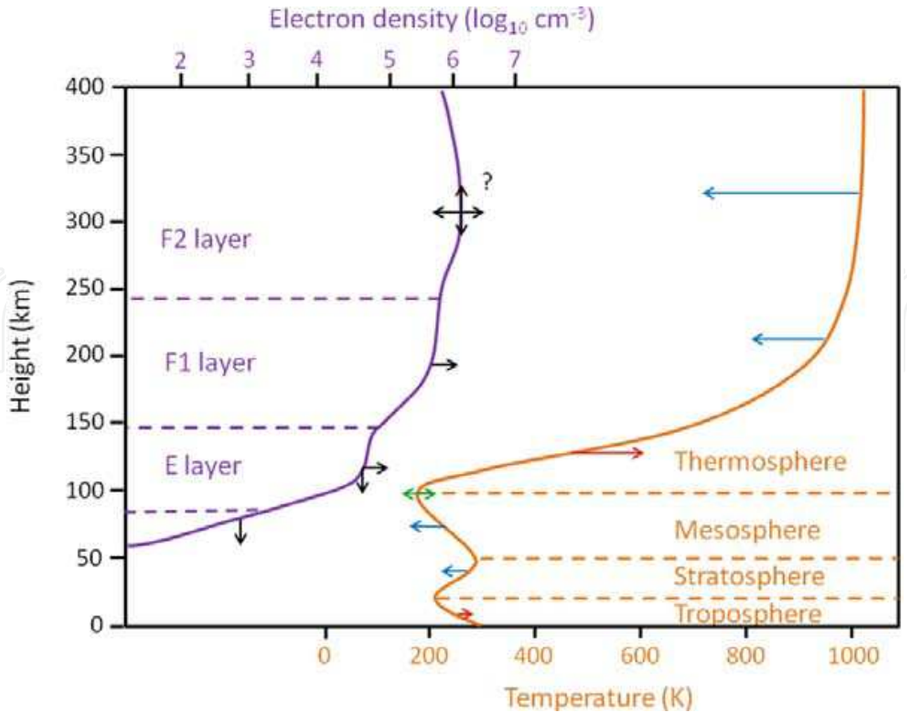

Fig. 1. Schematic summary of observed global mean trends in the atmosphere, after Laštovička et al. (2006a). Changes in the temperature profile (orange) are indicated by red (warming), blue (cooling) and green (no clear trend) arrows. Changes in the electron density profile (purple) are indicated by black arrows. Vertical arrows indicate the movement of the height of the peak electron density of the layer, while horizontal arrows indicate changes in the peak electron density itself. Trends in the F_2 layer vary strongly with location, season, and local time, so that no meaningful global mean can be defined. They are further discussed in section 2.4.

Beig et al. (2003) summarized temperature trends in the mesosphere. They reported that the lower and middle mesosphere has cooled on average by ~2-3 K/decade and at tropical latitudes the cooling trend increases with height in the upper mesosphere. However, near the mesopause the general consensus is that there is no significant trend. Some dependency of trends on latitude has been noted, but due to a limited number of sites, no clear pattern has yet emerged.

For the thermospheric temperature, only a few long-term trend studies are available. Semenov (1996) inferred a temperature trend of -30 K/decade based on changes in the atomic oxygen 630 nm emission layer, which is normally located at ~270 km. Holt & Zhang (2008) and Zhang et al. (2011) used incoherent scatter radar data from Millstone Hill (46.2°N, 288.5°E) to determine the long-term trend in ion temperature, which should be similar to the trend in neutral temperature, due to close thermal coupling between neutrals and ions. Zhang et al. (2011) showed that a warming trend is found between ~110 and 200 km altitude, and a cooling trend above 200 km, which increases with height and is stronger for lower solar activity. At 375 km the trend is as strong as -47±11 K/decade (Holt & Zhang, 2008). Donaldson et al. (2010), in a similar analysis of incoherent scatter

data from Saint Santin (44.1°N, 2.3°E), also found a warming at ~120-130 km of ~10 K/decade, and a cooling of -30 K/decade at 350 km, increasing with height. They also noted that negative trends were much larger at noon (up to -60 K/decade) than at midnight (nearly zero). For both locations trends were larger for the period from ~1980 onward.

2.3 Density

Because the atmosphere is nearly in hydrostatic equilibrium, a decrease in temperature results in contraction of the upper atmosphere, and a downward displacement of constant pressure surfaces. This means that the thermospheric density at a fixed height is expected to decrease. The same principle also explains why a warming is found in the lower thermosphere: as the thermosphere contracts the temperature profile essentially moves down. This results in an apparent warming at fixed height in the lower thermosphere due to the strong positive vertical gradient in temperature there (Akmaev & Fomichev, 1998).

Information about thermospheric density can be obtained from the orbits of near-Earth objects. Keating et al. (2000), Emmert et al. (2004, 2008), Emmert & Picone (2011), Marcos et al. (2005) and Saunders et al. (2011) used this technique and confirmed that the thermospheric density at fixed height is indeed decreasing. Observed trend magnitudes range from about -2%/decade to about -6%/decade, and generally increase with altitude. Trends are again larger for solar minimum conditions than for solar maximum conditions (Emmert et al., 2004). Emmert et al. (2008) reported that there is also a dependence on season, with trends being strongest in October and weakest in January and February. No dependence on local time or latitude was found.

2.4 Ionospheric trends

Another consequence of atmospheric contraction as a result of global cooling is that ionospheric layers are expected to move downward, as they tend to stay on the same pressure level. On the other hand, ion and electron densities should not be affected much as a result of global cooling, as both ion production rates and recombination coefficients are expected to be affected in a similar way (Rishbeth, 1990). Any increase in ion production should therefore mostly be offset by a similar increase in ion loss. Still, both long-term changes in the height of ionospheric layers and in their critical frequencies have been found.

Trends in the F_2 layer vary strongly with location, season, and local time. Bremer et al. (2004) reported median trends in f_oF_2 and h_mF_2, derived from over 50 ionospheric stations, of -0.01 MHz/decade and -0.09 km/decade, respectively. However, local trends tend to be much stronger and can be either positive or negative. Figure 2 shows trends in h_mF_2 at noon for May-June-July, colour-coded by strength, and demonstrates that trends of the order of ±1-5 km/decade are the most common of the trends that are considered reliable (filled circles). Both trends in h_mF_2 and f_oF_2 depend on the season and time of day (even switching sign), but this dependence is different for different stations (e.g. Elias & Ortiz de Adler, 2006). Similarly, no consistent dependence on solar activity level has been found (based on calculations by Th. Ulich, pers. comm., 2007).

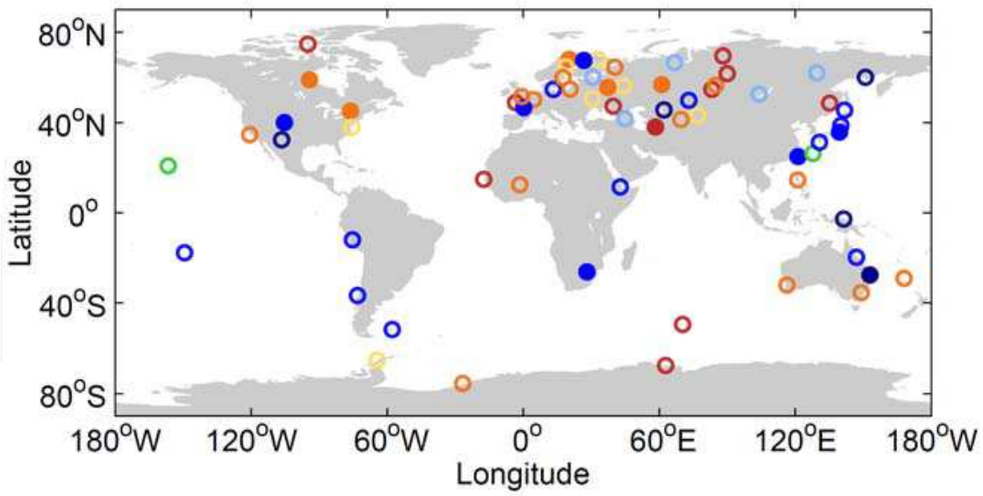

Fig. 2. Trends in h_mF_2 for May-June-July at noon hours (10-14 LT) colour-coded for strength. Dark blue: <-5 km/decade, medium blue: -5 to -1 km/decade, light blue: -1 to -0.2 km/decade, green: -0.2 to +0.2 km/decade, yellow: +0.2 to + 1 km/decade, orange: +1 to +5 km/decade, red: >5 km/decade. Filled circles represent trends that are larger than the standard deviation and were calculated based on at least 80 data points. They are therefore the most reliable. All other trends are represented by open circles. Trends were calculated using the Shimazaki (1955) formula by Th. Ulich (pers. comm., 2007).

Some studies have found regional patterns in F_2 layer trends. Danilov & Mikhailov (1999) found that the magnitude of trends in f_oF_2 increases with magnetic latitude. However, Bremer (1998) argued against this, and instead found a dependence on longitude: trends in both h_mF_2 and f_oF_2 were in general negative west of 30°E, but positive east of 30°E. Jarvis (2009) confirmed this finding. Bencze (2007, 2009) found that ionospheric stations showing negative trends in h_mF_2 are mostly located near seashores, while stations in continental areas usually exhibit positive trends.

3. Greenhouse gases and ozone

3.1 Background and mechanisms

3.1.1 Greenhouse gases

The CO_2 concentration in the Earth's atmosphere has increased from its estimated level of ~280 ppm before the industrial revolution to 317 ppm in 1960 and 390 ppm in 2010 as measured at ground level in Mauna Loa, Hawaii (P. Tans & R. Keeling, data obtained from www.esrl.noaa.gov/gmd/ccgg/trends, June 2011). The concentration of methane has also increased, from 1151 ppb in 1985 to 1355 ppb in 2008 as observed in the lower stratosphere (Rinsland et al., 2009). Partly as a result of the increase in methane, stratospheric water vapour has increased as well, by ~2 ppmv from 1945 to 2000, with its present-day level at ~4-6 ppmv (Rosenlof et al., 2001; Hurst et al., 2011).

CO_2, methane and water vapour all act as greenhouse gases. In the troposphere, greenhouse gases absorb outgoing infrared radiation, and emit it back to the surface, which results in warming. In the upper atmosphere they have the opposite effect. Greenhouse gases cool the

upper atmosphere, because they emit infrared radiation mostly to space upon relaxation from an excited state induced by collisions. This way they act to remove thermal energy from the upper atmosphere. This process overcomes the effects of extra absorption of radiation in the lower atmosphere, resulting in a net cooling effect. CO_2 is by far the most important contributor to infrared cooling in the middle atmosphere, followed by water vapour, while methane makes only a very small contribution (e.g. Fomichev, 2009). In the thermosphere both cooling by CO_2 and by nitric oxide (NO) is important.

3.1.2 Ozone

Ozone is also an important gas for the radiative budget of the stratosphere and mesosphere. Ozone absorbs solar ultraviolet (UV) radiation in the Chappuis (450-750 nm), Huggins (310-360 nm), and Hartley (450-750 nm) bands, which results in heating. The maximum heating occurs near the stratopause. Ozone also contributes to infrared cooling, but this is a much smaller effect (e.g. Fomichev, 2009).

The total ozone concentration decreased from ~375 Dobson units (DU) in 1970 to ~325 DU in 2000 as measured in Switzerland, with much stronger decreases occurring over the polar regions (Solomon, 1999). While the downward trend in ozone concentration may have slowed or even reversed in recent years (Stolarski & Frith, 2006; Salby et al., 2011), any data from the 1970s to the present-day will contain the effects that may have arisen from the original decrease in ozone concentration. A decrease in ozone results in less heating (i.e. cooling), and so acts in the same way as an increase in greenhouse gases. Note that while ozone is most important in the stratosphere and mesosphere, the cooling influence may still be felt in the thermosphere through the effect of atmospheric contraction.

3.1.3 Indirect effects

Once changes in temperature occur, whether they are caused by changes in greenhouse gases, ozone, or another process, this induces further indirect effects. We already noted that global cooling leads to thermal contraction, which has consequences for the density at a fixed height and the vertical electron density distribution. Changes in horizontal temperature structure can lead to changes in dynamics through changes in pressure gradients. The changes in dynamics can then cause further changes in temperature structure, and so on.

Not only the neutral atmosphere can be affected this way; ionospheric plasma transport is affected by changes in the neutral winds via ion-neutral collisions. Because the ionospheric plasma tends to be "frozen-in" to the magnetic field lines, meaning that it tends to flow along magnetic field lines, horizontal neutral winds can induce a vertical component in the plasma motion due to the inclination of magnetic field lines, as shown schematically in figure 3 (see also Rishbeth, 1998; Cnossen & Richmond, 2008). Due to the configuration of the Earth's magnetic field, ionospheric plasma is forced up magnetic field lines when neutral winds blow towards the magnetic equator, which acts to increase h_mF_2, and vice versa when neutral winds blow poleward. Because the geographic equator does not exactly coincide with the magnetic equator, not only the meridional wind, but also the zonal wind can contribute to the plasma transport taking place this way, although the contribution from

the meridional wind is dominant. Qian et al. (2009) have shown that this mechanism may be responsible for some of the spatial variation in trends in h_mF_2, as discussed in section 3.2.3.

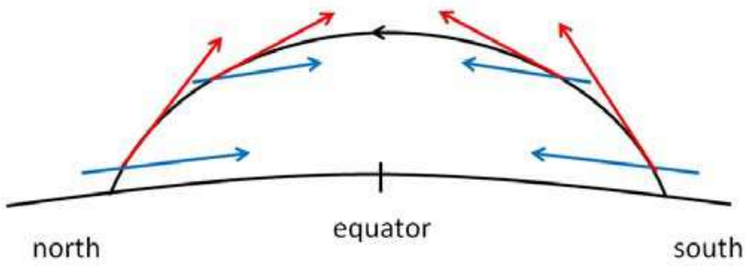

Fig. 3. Schematic illustration of the ionospheric plasma motion (red arrows) along a magnetic field line (black line with arrow) induced by horizontal neutral winds (blue arrows) blowing equatorward. In this case the ionospheric plasma is forced up magnetic field lines, resulting in an increase in h_mF_2. The opposite is true in case of poleward neutral winds. Note that the vertical component of the plasma motion becomes smaller near the equator, where the magnetic field makes a smaller angle with the Earth's surface.

3.2 Effect estimates and comparison to observations

3.2.1 Temperature

Roble & Dickinson (1989) were the first to quantify the effect of an increase in greenhouse gases on the upper atmosphere. They used a 1-D model of the upper atmosphere to show that a doubling of the CO_2 and methane concentration would cause a cooling of the thermosphere of up to 50 K. Since this initial pioneering study, many more have followed, using increasingly sophisticated numerical models of the upper atmosphere.

Most modelling studies employed a doubling of the CO_2 concentration, like Roble & Dickinson (1989). This can make it somewhat difficult to make direct quantitative comparisons between observed and modelled trends, as a doubling has not yet occurred. When variables depend more or less linearly on the CO_2 concentration, such as the thermospheric temperature or h_mF_2 (Cnossen, 2009; Cnossen et al., 2009), modelling results can be linearly interpolated. However, the response in thermospheric density decreases with increasing CO_2 concentration, so that linear interpolation results in an underestimate of trends (Cnossen, 2009).

Akmaev & Fomichev (2000) avoided such problems by performing simulations with the Spectral Mesosphere/Lower Thermosphere Model (SMLTM; Akmaev et al., 1992), using the CO_2 concentrations of 1955 and 1995 (313 and 360 ppm, respectively). The global mean vertical profile of the thermal response they found was in qualitative agreement with observations, showing cooling in the mesosphere, little change near the mesopause, a slight warming in the lower thermosphere, and a cooling from ~120-125 km that increased with height. However, their mesospheric cooling was about -0.8 K/decade, ~3 times smaller than observed. Also the thermospheric cooling was smaller than observed, and the turning point from warming to cooling in the lower thermosphere occurred at too low altitude.

Akmaev et al. (2006) therefore performed additional model simulations with the SMLTM which included also changes in water vapour and ozone concentration. The inclusion of

ozone resulted in a much stronger modelled cooling in the mesosphere of nearly 2 K/decade, almost as strong as the observed trend. The addition of ozone, and to a lesser extent water vapour, also produced a more pronounced warming in the lower thermosphere of up to 3 K/decade at ~115 km, which turned into a cooling again above ~150 km.

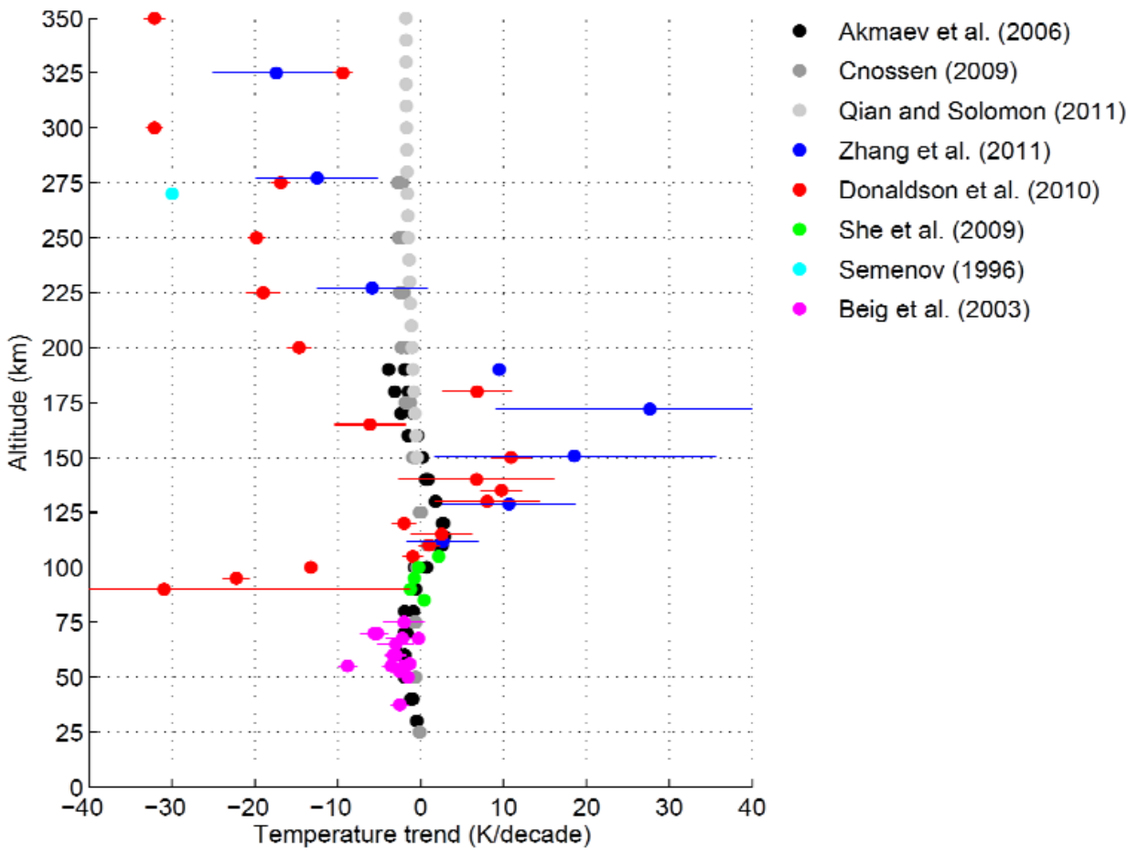

Fig. 4. Observed and modelled temperature trends (dots) with error bars where available (lines). Note that modelling results are in black/grey while observational results are in colour. For Akmaev et al. (2006) both January and March results are shown (stronger trends are for January) and for Cnossen (2009) both March and June results are shown (stronger trends are for June, though there is only a small difference). All other results are seasonal averages.

Cnossen (2009) obtained results similar to those of Akmaev et al. (2006) using simulations with the Coupled Middle Atmosphere and Thermosphere Model 2 (CMAT2; Harris, 2006), studying the combined effects of changes in CO_2 and ozone concentration between 1965 and 1995. Qian et al. (2006) and Qian & Solomon (2011) used a global mean model to investigate trends higher up in the thermosphere, but considered only changes in the CO_2 concentration from 1970 to 2000.

The temperature trends calculated by Akmaev et al. (2006), Cnossen (2009) and Qian & Solomon (2011) are compared to observed trends in figure 4. There is good agreement

between the Akmaev et al. (2006) and Cnossen (2009) model estimates and observed trends in the middle atmosphere and lower thermosphere (25-120 km). However, at ~130-180 km, most observations show a strong apparent warming, which is not reproduced by the models. Also, the strong cooling observed higher up in the thermosphere (>200 km) is underestimated by the modelling studies by Cnossen (2009) and Qian & Solomon (2011). Both studies predict a cooling that remains more or less constant with increasing altitude (>200 km), while observations indicate a strengthening of the trend with increasing altitude.

Akmaev et al. (2006) argued that the lack of a strong warming in the lower thermosphere in their results might be due to an overestimate of the amount of CO_2 present in the upper mesosphere and lower thermosphere in the SMLTM. Still, this does not explain why too little cooling is predicted by modelling studies above ~200 km. Although the observed thermospheric temperature trends are based on data from just two sites, it does appear that changes in CO_2 and ozone concentration cannot fully explain those trends.

3.2.2 Density

The same modelling studies described in the previous section also provided trends in density, which are compared to each other and to observations in figure 5. The density trends modelled by Akmaev et al. (2006) are about twice as strong as those modelled by Cnossen (2009). However, there is also a large spread in observed trends. At ~200 km, the Akmaev et al. (2006) trends seem to agree quite well with trends observed by Saunders et al. (2011), while the Cnossen (2009) trends agree better with Emmert & Picone (2011) and Emmert et al. (2004). The trends modelled by Qian & Solomon (2011) at higher altitude also tend to agree best with Emmert & Picone (2011) and Emmert et al. (2004), as well as Marcos et al. (2005).

Depending on which observations and modelling results are chosen for comparison, it may be argued that trends in density show better agreement between models and observations than trends in temperature. However, this may be partly so because the density at a certain height responds to the temperature structure of the entire atmosphere below. That means that the effects of insufficient warming below 200 km and insufficient cooling above 200 km could to some extent cancel each other out at altitudes above 200 km.

The modelled seasonal dependence of trends in density does not match with observations. Emmert et al. (2008) found that density trends are weakest in January and February, while the modelled trends by Akmaev et al. (2006) are stronger for January than for March. Changes in CO_2 and ozone concentration can therefore not explain the observed seasonal dependence.

There is however an explanation for the dependence of trends in density and temperature on the solar activity level. Qian et al. (2006) showed that stronger trends during solar minimum are due to CO_2 cooling being a relatively more important cooling mechanism at solar minimum, while cooling by nitric oxide (NO) becomes more important at solar maximum. A change in CO_2 concentration therefore has a larger impact on the radiative balance in the upper atmosphere during solar minimum than during solar maximum.

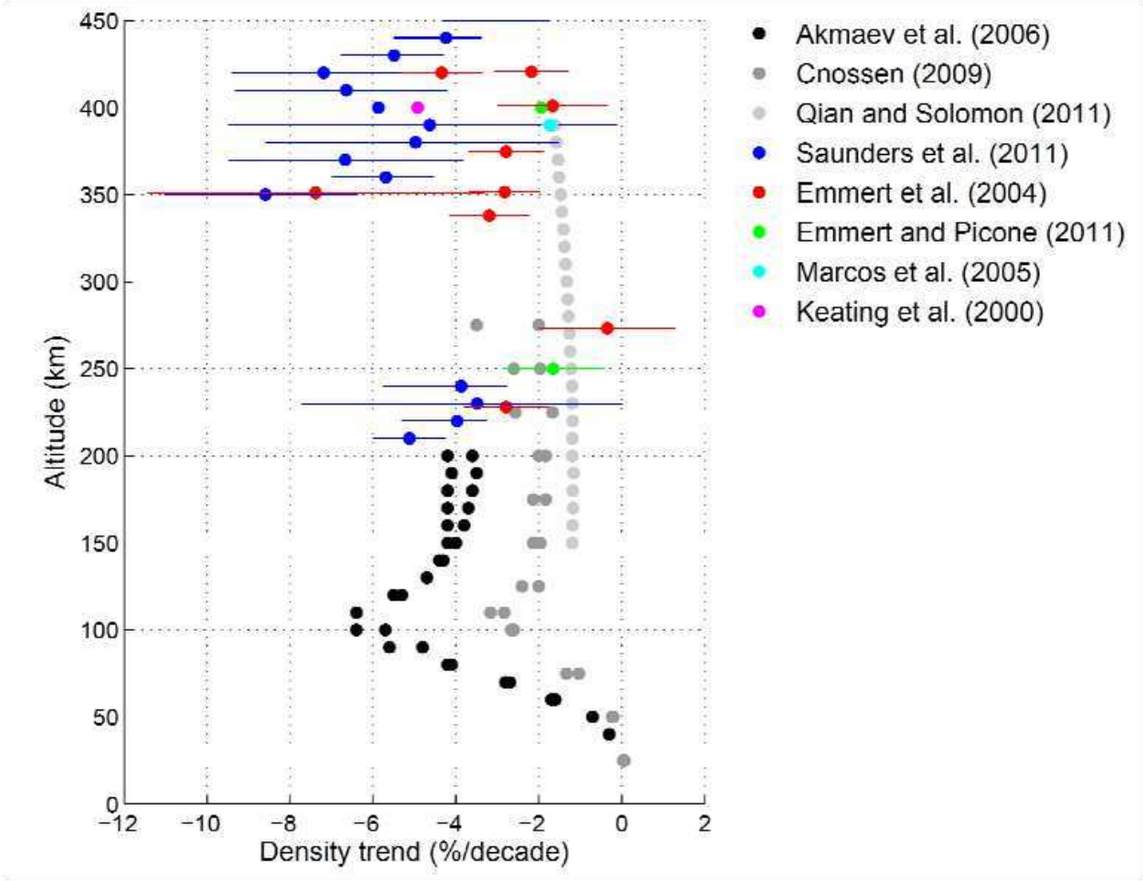

Fig. 5. Observed and modelled density trends (dots) with error bars where available (lines) Note that modelling results are in black/grey while observational results are in colour. For Akmaev et al. (2006) both January and March results are shown (stronger trends are for January) and for Cnossen (2009) both March and June results are shown (stronger trends are for June). All other results are seasonal averages.

3.2.3 The ionospheric F_2 layer

Qian et al. (2009) performed simulations with the Thermosphere-Ionosphere-Electrodynamics General Circulation Model (TIE-GCM; Roble et al., 1998; Richmond et al., 1992), focusing more on the effects of CO_2 cooling on the F_2 layer ionosphere. They doubled the CO_2 concentration from 365 ppmv to 730 ppmv and noted that certain features of the changes in N_mF_2 and h_mF_2 followed the magnetic equator, indicating the role of electrodynamics in generating these trends.

Qian et al. (2009) showed that changes in both the meridional and zonal neutral wind affected the transport of ionospheric plasma by neutral winds, through the mechanism described in section 3.1.3. This was an important contributor to changes in h_mF_2, especially under solar minimum conditions. At solar maximum, they found that the changes in N_mF_2 matched quite well with the pattern of changes in the O/N_2 ratio, which is proportional to the balance of ion production and loss rates. This result indicated a less important role for

changes in dynamics, and Qian et al. (2009) found indeed that changes in neutral winds were smaller at solar maximum. The smaller changes found under solar maximum conditions could again be linked to the smaller contribution to the radiative budget of CO_2 cooling relative to NO cooling at solar maximum (Qian et al., 2006).

The changes in h_mF_2 modelled by Qian et al. (2009) were mostly negative, as expected, but they were occasionally positive for solar minimum, usually after midnight. To compare the magnitude of the changes they found to observed trends, figure 6 shows trends in h_mF_2 and f_oF_2 in km/decade and MHz/decade, linearly interpolated from their results for 3 LT. The interpolation was done based on the actual change in CO_2 concentration between 1960 and 2010 (73 ppm; 14.6 ppm/decade), so that their original numbers were divided by 25 (365/14.6).

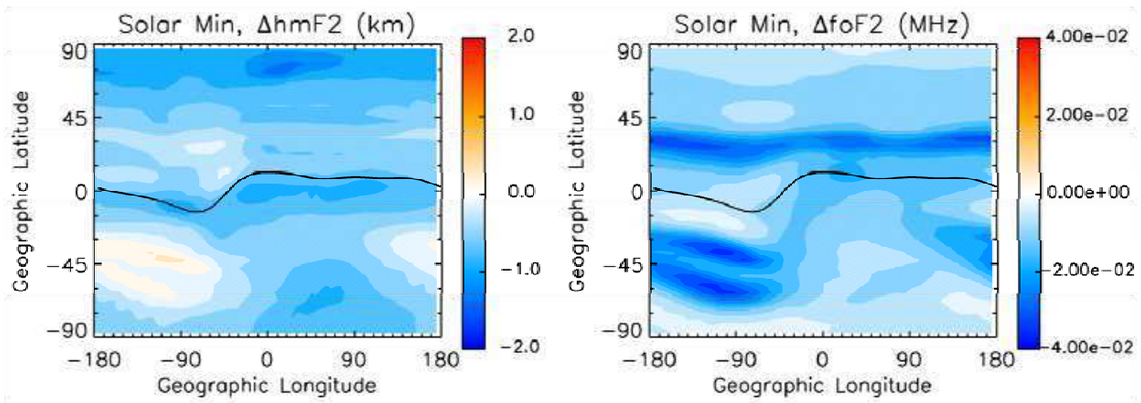

Fig. 6. Trends in h_mF_2 in km/decade (left) and f_oF_2 in MHz/decade (right) at 3 LT linearly interpolated from the model simulations by Qian et al. (2009) at June solstice.

A typical interpolated trend in h_mF_2 is -1 km/decade, while maximum negative trends go up to about -2 km/decade (at 12 LT; not shown) and maximum positive trends up to 0.5 km/decade. These values are somewhat larger than the median change in h_mF_2 reported by Bremer et al. (2004), but ~2-5 times smaller than typical changes at individual stations. Modelled trends for solar maximum conditions are even smaller. Estimated trends in f_oF_2 vary between 0 and -0.04 MHz/decade. The strongest trend of -0.04 MHz/decade is also larger than the median change in f_oF_2 of -0.01 MHz/decade reported by Bremer et al. (2004), but again underestimates changes observed at many individual stations. Positive trends that have been reported in some locations are not explained at all. From these results we can conclude that the change in CO_2 concentration has contributed to long-term trends in the F_2 layer, but it is unlikely to be the sole cause.

4. Secular variation of the Earth's magnetic field

4.1 Background and mechanism

The Earth's magnetic field varies slowly in strength and in orientation over time, and also the relative contributions of the main dipole component and higher order field components vary. We are currently at a time of relatively strong change in terms of field intensity, as the Earth's dipole moment has decreased by about 5% per century since 1840, while little

change in field strength occurred from 1590 to 1840 (Gubbins et al., 2006). The angle between the geomagnetic dipole and the Earth's rotation axis, the tilt angle, has changed also over the last half century, from ~11.7° in 1960 to ~10.5° in 2005, following more than a century where it remained nearly constant (Amit & Olson, 2008).

The Earth's magnetic field plays a role in the state of the upper atmosphere in various ways. First of all, it is what shapes the Earth's magnetosphere, and controls to some extent the interactions of the magnetosphere with the solar wind and the ionosphere. This determines the flux and energy of energetic particles precipitating into the upper atmosphere, as well as the high-latitude electric field and ionospheric convection pattern (see e.g. Kivelson & Russell (1995) for further details).

Secondly, the orientation of the Earth's magnetic field influences the transport of ionospheric plasma by neutral winds. This process has been described in section 3.1.3 in the context of indirect effects of changes in circulation. However, even if there were no changes in the neutral wind, changes in the inclination and declination of the Earth's magnetic field could still cause changes in the plasma motion. The inclination is the angle between the magnetic field and the Earth's surface and the declination is the angle with geographic North. A change in the inclination I directly affects the vertical component of the plasma motion driven by neutral winds, which is equal to the component of the horizontal neutral wind parallel to the magnetic field, $v_{n,par}$, times the factor $\sin(I)\cos(I)$. A change in declination changes the magnitude of $v_{n,par}$, as it changes the projection of the neutral wind onto magnetic field lines. The changes in magnetic field orientation also cause changes to the ion drag acting on the neutral wind, so that neutral winds are likely to change as well.

The neutral wind is also responsible for the generation of the dynamo electric field $\mathbf{E}_{dyn}$ through $\mathbf{E}_{dyn} = \mathbf{v}_n \times \mathbf{B}$, where $\mathbf{v_n}$ is the neutral wind and $\mathbf{B}$ the magnetic field. Both changes in the neutral wind and changes in declination and inclination alter the component of $\mathbf{v}_n$ perpendicular to $\mathbf{B}$. In addition, a change in the magnitude of $\mathbf{B}$ changes the ionospheric Pedersen and Hall conductivities, and these combined effects induce a change in the electrostatic field $\mathbf{E}$. The change in $\mathbf{E}$ and $\mathbf{B}$ does not only cause changes to the ion drag exerted on the neutral wind, further modifying $\mathbf{v}_n$, but also modifies the $\mathbf{E}\times\mathbf{B}$ drift of ions and electrons. The vertical component of this drift can be expected to change h_mF_2 and f_oF_2 too.

While the ionosphere is expected to be most directly affected by changes in the magnetic field, changes to the neutral atmosphere can occur as well. Possible effects on the neutral wind via ion-neutral collisions have already been mentioned, and as noted before, any changes in circulation can have secondary effects on for instance the neutral temperature structure. The neutral temperature in the thermosphere may also be directly affected through changes in Joule heating.

4.2 Effect estimates and comparison to observations

Cnossen & Richmond (2008) quantified the global effects of magnetic field changes on the ionospheric F_2 layer using simulations with the Thermosphere-Ionosphere-Electrodynamics general circulation model (TIE-GCM). They found that changes in the Earth's magnetic field from 1957 to 1997 had a substantial effect on h_mF_2 and f_oF_2 in some parts of the world, primarily South America and the southern Atlantic Ocean (see figure 7). In these regions,

the inclination of the magnetic field changed the most. The changes in inclination were the dominant cause of the trends in the F_2 layer, by changing plasma transport up and down magnetic field lines driven by neutral winds. Neutral winds also changed somewhat, but no significant effects on the thermospheric temperature were found.

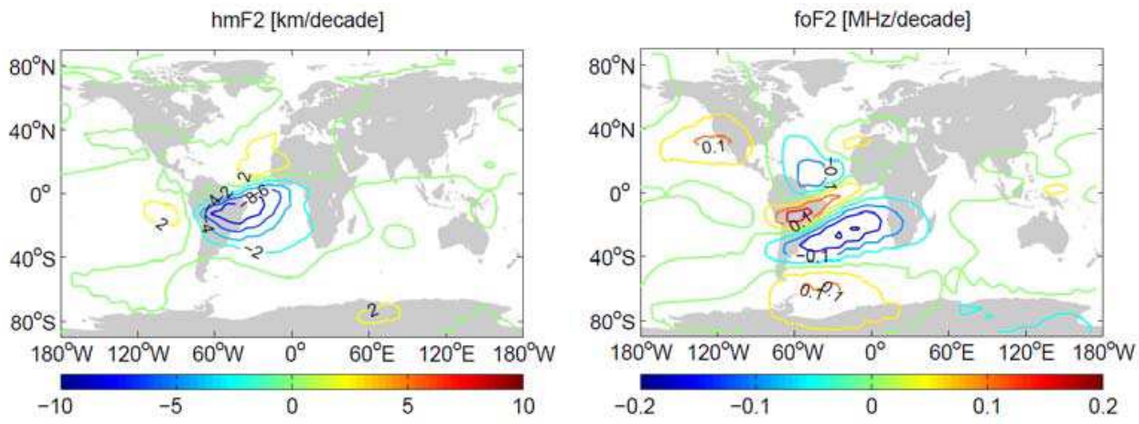

Fig. 7. Trends in h_mF_2 in km/decade (left) and f_oF_2 in MHz/decade (right) at 12 LT at June solstice due to changes in the Earth's magnetic field, interpolated from the model simulations by Cnossen & Richmond (2008).

Figure 7 shows the average trends in h_mF_2 and f_oF_2 in km/decade and MHz/decade, respectively, linearly interpolated from the change between 1957 and 1997. Over South America and the southern Atlantic Ocean, modelled trends in h_mF_2 and f_oF_2 are of the order of -5 to +2 km/decade and ±0.1 MHz/decade, respectively. Trends show a strong spatial dependence, and also vary (even in sign) depending on the season and time of day.

The magnitudes of the trends due to magnetic field changes in the regions that are most strongly affected are quite similar to the magnitudes of typical observed trends, and 2-5 times larger than the maximum changes predicted to be caused by changes in the CO_2 concentration. Still, a direct comparison between modelled and observed trends at specific stations indicated that modelled trends were usually smaller. At Concepción (36.8°S, 73.0°W) and Argentine Islands (65.2°S, 64.3°W), both located in the region where modelled trends were strongest, changes in the magnetic field could account for ~30-50% and ~20% of the observed trends. The observed and modelled seasonal-diurnal patterns of trends for these stations did not match.

The predicted changes outside the region of South America and the southern Atlantic Ocean were very small. However, the spatial pattern of modelled trends, showing a marked change at a longitude of ~0-20°, with weak trends east of that line, and much stronger trends to the west, was somewhat similar to the findings of Bremer (1998) and Jarvis (2009), although they found positive trends west of 30° and negative trends east of 30°. An increase of f_oF_2 trends with geomagnetic latitude, as found by Danilov & Mikhailov (1999), was not found.

Based on the study by Cnossen & Richmond (2008) we can conclude that long-term changes in the magnetic field are important in some regions, but do not explain observed trends elsewhere. However, Cnossen & Richmond (2008) had to neglect any effects of changes in

the high-latitude coupling between the magnetosphere and ionosphere-thermosphere system that might arise, as their model did not include a magnetosphere. This could have resulted in an underestimation of the effects of magnetic field changes, especially at high latitudes.

Recently the TIE-GCM has been successfully coupled to the Lyon-Fedder-Mobarry (LFM) MHD code, forming the Coupled Magnetosphere-Ionosphere-Thermosphere (CMIT) model (Wiltberger et al., 2004; Wang et al., 2004, 2008). With this model it is now possible to include the effects of changes in high-latitude magnetosphere-ionosphere coupling, and Cnossen et al. (2011) have started to use this to re-assess the effects of changes in the magnetic field on the ionosphere and thermosphere.

Cnossen et al. (2011) started with a simplified experiment, investigating the effect of changes in magnetic field strength only. They reduced the magnetic field strength to 75% of its present-day value, which caused changes in h_mF_2 of up to -40 and +60 km and changes in f_oF_2 of up to -3 to +1 MHz. If a linear response is assumed, considering a 5% decrease in magnetic field strength per century, these would be equivalent to trends of -0.8 to +1.2 km/decade and -0.06 to +0.02 MHz/decade. While clearly smaller than the trends predicted from the full magnetic field changes between 1957 and 1997, as expected, this rough estimate indicates that changes in magnetic field strength alone could still make a significant contribution to long-term trends. The trends in h_mF_2 and f_oF_2 predicted in this way appear to be of similar order of magnitude as those due to changes in CO_2 concentration.

The spatial pattern of changes simulated by CMIT is different from that simulated with TIE-GCM for the full magnetic field changes between 1957 and 1997, which is perhaps not surprising, as they were caused (predominantly) by different mechanisms. The new experiments show strong changes in h_mF_2 over Australia, the Pacific Ocean, and the northern Indian Ocean, and smaller changes over the Atlantic Ocean. This opens up the possibility that effects of changes in the magnetic field are present over different and more widespread areas than previously thought. A detailed comparison between the changes modelled by CMIT and observed trends will be done once CMIT simulations with historic magnetic fields have been performed, which are planned for the near future.

5. Changes in solar and geomagnetic activity

5.1 Solar activity

The solar activity level varies over an approximately 11-year cycle, and there are indications that there are longer-term variations too (e.g. Pap & Fox, 2004). When the Sun is more active, it is brighter and emits more radiation, especially in the shorter wavelengths, such as the ultraviolet (UV) and extreme ultraviolet (EUV), which are important for the radiative budget of the middle and upper atmosphere. Absorption of EUV radiation also results in ionization of O, O_2, and N_2. Any long-term changes in solar activity may therefore be expected to cause long-term trends in the temperature and electron density distribution in the upper atmosphere.

Lean (2001) used EUV satellite measurements and proxies (proxies only before 1974) to study long-term trends in EUV irradiance, and found an increase over the first half of the 20th century, with no clear trend after 1950. Since most observed trends in the upper atmosphere have been derived from data collected after 1950, a long-term trend in solar

activity is unlikely to have contributed much to those (Laštovička, 2005). However, for other time intervals (e.g. 1900-1950) it could be a contributor.

5.2 Geomagnetic activity

Geomagnetic activity is a manifestation and measure of "space weather", arising from the interaction between the solar wind and the Earth's magnetosphere. This interaction generates currents in the ionosphere and magnetosphere which cause small perturbations to the main magnetic field of the Earth that can be measured at the surface. These magnetic perturbations form the basis of indices of geomagnetic activity, such as the Ap, aa, and Kp indices. Each of these indices is derived from the K index, which is related to the maximum fluctuations of the horizontal components of the observed geomagnetic field, relative to a quiet day (a day with few disturbances due to the solar wind), during a three-hour interval.

Various studies have indicated the presence of a long-term trend in geomagnetic activity over the past ~50-150 years. Clilverd et al. (1998) and Stamper et al. (2002) found that the geomagnetic activity in terms of the aa-index was increasing throughout the 20th century, and Clilverd et al. (2002) found that the number of geomagnetic storms per solar cycle had also been increasing until it stabilized in the last few cycles. Long-term changes in the solar quiet-time day variation, Sq, have been found as well. Macmillan & Droujinina (2007) reported a weak upward trend of on average 1.3 nT per century (~10%) in the Sq amplitude based on records from 14 magnetic observatories. Elias et al. (2010) analysed data from three stations, and found also positive trends in Sq of 5-10%/century.

High geomagnetic activity indicates disturbed space weather conditions, usually resulting from disturbances in the solar wind. This tends to lead to stronger energetic particle precipitation and ionospheric convection at high latitudes, stronger ionospheric currents, and an enhancement of the Joule heating in the upper atmosphere, eventually leading to higher temperatures and stronger neutral winds. Variations in geomagnetic activity occur on short timescales from minutes to days, and are responsible for part of the large natural variability in the thermosphere-ionosphere system. A gradual, long-term change in the background level of geomagnetic activity could therefore cause a long-term trend in the upper atmosphere.

Because geomagnetic activity is a measure of the interaction between the solar wind and the Earth's magnetosphere-ionosphere-thermosphere system, the origin of long-term changes in geomagnetic activity could be associated either with the Sun (e.g. Stamper et al., 1999) or with the terrestrial system (or both). Clilverd et al. (2002) concluded from a simple calculation that involved various assumptions and approximations that changes in the Earth's magnetic field would have little effect on geomagnetic activity. However, a detailed analysis has not been done yet, and the simulations by Cnossen et al. (2011) indicate that the effect may be larger than previously thought, due to a stronger dependence of the ionospheric conductance on the magnetic field strength than was assumed by Clilverd et al. (2002). When considering the effects of changes in geomagnetic activity on the upper atmosphere, it is therefore possible that these may ultimately be due to changes in the Sun and/or changes in the Earth's magnetic field. Nevertheless, the effect of the observed change in geomagnetic activity on the upper atmosphere, regardless of which processes may have contributed to it, can still be investigated.

Laštovička (2005) claims that the role of geomagnetic activity in causing long-term trends was small for the second half of the 20th century, just like that of solar activity. However, there has been little effort so far to actually quantify the effect of reported long-term changes in geomagnetic activity on the upper atmosphere. No detailed modelling study exists, so this may be an area for future studies to explore.

6. Influences from the lower atmosphere

The lower atmosphere influences the upper atmosphere through upwardly propagating planetary waves, gravity waves and tides, and acts in general as a boundary condition for the middle and upper atmosphere. Any long-term changes in the lower atmosphere therefore have the potential to induce long-term changes in the upper atmosphere.

Jarvis (2009) argued that the longitudinal variation in h_mF_2 trends over Eurasia found by himself and Bremer (1998) suggests the influence of a stationary wave-like feature between 3°W and 104°E, and that the fact that it is a geo-stationary feature implies a cause linked to the troposphere or solid Earth. On this basis, he proposed that the longitudinal variation in F_2 region trends might be caused via long-term changes in non-migrating tides, originating in the troposphere. Bencze (2007, 2009) also proposed an influence of non-migrating tides to explain differences in h_mF_2 trends between continental regions and oceans/seashores. Note that "non-migrating" in this context means "not moving with the apparent motion of the Sun".

It has been found that in particular the eastward propagating zonal wavenumber-3 diurnal tide (DE-3) has a strong influence on the ionosphere and thermosphere, especially at low latitudes (Hagan & Forbes, 2002). The DE-3 tide originates in the tropical troposphere primarily through latent heat release associated with deep convective cloud systems. Forbes et al. (2006) explained that this process is intimately connected with the predominant wavenumber-4 longitudinal distribution of topography and land-sea differences at low latitudes. The interaction of the diurnal harmonic of solar radiation with the characteristics of the Earth's surface, roughly displaying a wavenumber-4 pattern, generates the DE-3 tide. From a Sun-synchronous perspective, this appears to the observer as a wavenumber-4 feature mimicking the longitudinal surface heating pattern (Forbes & Hagan, 2000).

Wavenumber-4 patterns in the thermosphere and ionosphere have indeed been observed (e.g. Immel et al., 2006; Häusler et al., 2007). Hagan et al. (2007) performed simulations with the TIME-GCM, using a lower boundary tidal forcing from the Global Scale Wave Model (GSWM; Hagan & Forbes, 2002), which includes only latent heat release as a source of non-migrating tides. This confirmed that the DE-3 tide generated this way propagates all the way up into the thermosphere, where it excites a wavenumber-4 longitudinal structure, similar to observations. Jarvis (2009) noted that observed wavenumber-4 patterns in the thermosphere have a scale size similar to that of the longitudinal variations found in long-term trends in h_mF_2. It may therefore be that long-term changes in tropical convection could be ultimately responsible for at least part of the long-term change in the ionosphere.

Unfortunately, the ionospheric data currently available are not evenly spread over the globe, and therefore are insufficient to determine whether the longitudinal variation found between 3°W and 104°E is part of a global wavenumber-4 pattern. In addition, there is insufficient information on non-migrating tides to determine whether they exhibit long-term trends, let alone whether these would be large enough to produce the ionospheric trends

that are observed. A direct test of this hypothesis is therefore not yet possible, but it remains an intriguing possibility.

7. Conclusion

Temperature trends in the mesosphere can be explained largely by changes in CO_2 and ozone concentration. The effect of changes in water vapour concentration is much smaller. Observed changes in the thermospheric temperature have not been fully explained by model simulations of compositional changes. They mostly have the expected sign, but are not strong enough. Estimated trends in h_mF_2 and f_oF_2 are also 2-5 times smaller than what is typically observed.

There are several possible explanations for the discrepancies between modelled and observed trends in the thermosphere. There are errors associated with the data (see section 2.1 and figures 3 and 4), and also the models do not represent reality perfectly. There is for instance some uncertainty over the collisional excitation rate between CO_2 and atomic oxygen, which determines the efficiency of CO_2 cooling. The value chosen will affect the sensitivity in the model to changes in the CO_2 concentration, and there are many other factors that can have an influence too. Still the difference in magnitude between modelled and observed trends in the thermosphere is sufficiently large to suggest that thermospheric trends are not caused by changes in CO_2 and ozone concentration alone.

Indeed, simulations have shown that changes in the Earth's magnetic field also affect the F_2 layer. An initial study by Cnossen & Richmond (2008) showed that this is primarily important over South America and the southern Atlantic Ocean, while more recent simulations indicate that other regions may be affected too, even if only changes in magnetic field strength are considered. Detailed comparisons between modelled and observed trends are needed to determine to what extent changes in the magnetic field can explain the observations in the F_2 layer. Changes in the magnetic field do not explain trends in neutral temperature and density.

Further work is needed to get quantitative estimates of the effects of changes in geomagnetic activity level, and possible influences of long-term changes in the lower atmosphere. Also, in order to reduce the error bars on observed trends and detect any changes in trends that may occur over time, continued monitoring of the upper atmosphere, with as much global coverage as possible, is essential.

8. Acknowledgment

I would like to thank Shunrong Zhang, Bill Oliver, John Emmert, Arrun Saunders and Rashid Akmaev for sending me their data used in creating figures 4 and 5, Liying Qian for creating figure 6 for me, and Thomas Ulich for calculating the trends in h_mF_2. I am also grateful to Bill Oliver, Art Richmond, John Emmert, and Liying Qian for helpful feedback on an earlier version of this manuscript. The National Center for Atmospheric Research is sponsored by the National Science Foundation.

9. References

Akmaev, R.A., Fomichev, V.I., Gavrilov, N.M., & Shved, G.M. (1992). Simulation of the zonal mean climatology of the middle atmosphere with a 3-dimensional spectral

model for solstice and equinox conditions. *J. Atmos. Solar-Terr. Phys.*, Vol. 54, No. 2, pp. 119-128.

Akmaev, R.A., & Fomichev, V.I. (1998). Cooling of the mesosphere and lower thermosphere due to doubling of CO_2. *Ann. Geophys.*, Vol. 16, pp. 1501-1512.

Akmaev, R.A., & Fomichev, V.I. (2000). A model estimate of cooling in the mesosphere and lower thermosphere due to the CO_2 increase over the last 3-4 decades. *Geophys. Res. Lett.*, Vol. 27, No. 14, pp. 2113-2116.

Akmaev, R.A., Fomichev, V.I., & Zhu, X. (2006). Impact of middle-atmospheric composition changes on greenhouse cooling in the upper atmosphere. *J. Atmos. Solar-Terr. Phys.*, Vol. 68, No. 17, pp. 1879-1889.

Amit, H. & Olson, P. (2008). Geomagnetic dipole tilt changes induced by core flow. *Phys. Earth Plan. Interiors*, Vol. 166, No. 3-4, pp. 226-238.

Baldwin, M.P., & Dunkerton, T.J. (2001). Stratospheric harbingers of anomalous weather regimes. *Science,* Vol. 294, No. 5542, pp. 581-584.

Beig, G., Keckhut, P., Lowe, R.P., et al. (2003). Review of mesospheric temperature trends. *Rev. Geophys.*, Vol. 41, No. 4, 1015.

Bencze, P. (2007). What do we know of the long-term change of the Earth's ionosphere? *Adv. Space Res.*, Vol. 40, pp. 1121-1125.

Bencze, P. (2009). Geographical distribution of long-term changes in the height of the maximum electron density of the F region: A nonmigrating tide effect? *J. Geophys. Res.*, Vol. 114, A06304.

Bremer, J. (1998). Trends in the ionospheric E and F regions over Europe. *Ann. Geophys.*, Vol. 16, pp. 986-996.

Bremer, J., Alfonsi, L., Bencze, P., Laštovička, J., Mikhailov, A.V., & Rogers, N. (2004). Long-term trends in the ionosphere and upper atmosphere parameters, *Annals of Geophysics*, Vol. 47 (supplement), No. 2-3, pp. 1009-1029.

Clilverd, M.A., Clark, T.D.G., Clarke, E., & Rishbeth, H. (1998), Increased magnetic storm activity from 1868 to 1995, *J. Atmos. Solar-Terr. Phys.*, Vol. 60, pp. 1047-1056.

Clilverd, M.A., Clark, T.D.G., Clarke, E., Rishbeth, H., & Ulich, T. (2002). The causes of long-term changes in the aa index. *J. Geophys. Res.*, Vol. 107, No. A12, 1441.

Clilverd, M.A., Ulich, T., & Jarvis, M.J. (2003). Residual solar cycle influence on trends in ionospheric F2-layer peak height. *J. Geophys. Res.*, Vol. 108, No. A12, 1450.

Cnossen, I., & Richmond, A.D. (2008). Modelling the effects of changes in the Earth's magnetic field from 1957 to 1997 on the ionospheric hmF2 and foF2 parameters. *J. Atmos. Solar-Terr. Phys.*, Vol. 70, No. 11-12, pp. 1512-1524.

Cnossen (2009). *Modelling of long-term trends in the middle and upper atmosphere*. PhD thesis, University of Leicester, Leicester, UK.

Cnossen. I., Harris, M.J., Arnold, N.F., & Yiğit, E. (2009). Modelled effect of changes in the CO_2 concentration on the middle and upper atmosphere: Sensitivity to gravity wave parameterization, *J. Atmos. Solar-Terr. Phys.*, Vol. 71, pp. 1484-1496.

Cnossen, I., Richmond, A.D., Wiltberger, M., Wang, W., & Schmitt, P. (2011). The response of the coupled magnetosphere-ionosphere-thermosphere system to a 25% reduction in the dipole moment of the Earth's magnetic field. *J. Geophys. Res.*, in press.

Danilov, A.D. & Mikhailov, A.V. (1999). Spatial and seasonal variations of the foF2 long-term trends. *Ann. Geophys.*, Vol. 17, No. 9, pp. 1239-1243.

Donaldson, J.K., Wellman, T.J., & Oliver, W.L. (2010), Long-term change in thermospheric temperature above Saint Santin, *J. Geophys. Res.*, Vol. 115, A11305.

Elias, A.G., de Artigas, M.Z., & de Haro Barbas, B.F. (2010), Trends in the solar quiet geomagnetic field variation linked to the Earth's magnetic field secular variation and increasing concentrations of greenhouse gases, *J. Geophys. Res.*, Vol. 115, No. 8, A08316, doi: 10.1029/2009JA015136.

Elias, A.G., & Ortiz de Adler, N. (2006). Earth magnetic field and geomagnetic activity effects on long-term trends in the F2 layer at mid-high latitudes. *J. Atmos. Solar-Terr. Phys.*, Vol. 68, No. 17, 1871-1878.

Emmert, J.T., Picone, J.M., Lean, J.L., & Knowles, S.H. (2004). Global change in the thermosphere: compelling evidence of a secular decrease in density. *J. Geophys. Res.*, Vol. 109, No. A2, A02301.

Emmert, J.T., Picone, J.M., & Meier, R.R. (2008). Thermospheric global average density trends, 1967-2007, derived from orbits of 5000 near-Earth objects. *Geophys. Res. Lett.*, Vol. 35, No. 5, L05101.

Emmert, J.T. & Picone, J.M. (2011). Statistical uncertainty of 1967-2005 thermospheric density trends derived from orbital drag. *J. Geophys. Res.*, in press, doi.: 10.1029/2010JAO16382.

Fomichev, V.I. (2009). The radiative energy budget of the middle atmosphere and its parameterization in general circulation models. *J. Atmos. Solar-Terr. Phys.*, Vol. 71, pp. 1577-1585.

Forbes, J.M, & Hagan, M.E. (2000). Diurnal Kelvin wave in the atmosphere of Mars: Towards an understanding of 'stationary' density structures observed by the MGS accelerometer. *Geophys. Res. Lett.*, Vol. 27, No. 21, pp. 3563-3566.

Forbes, J.M., Russell, J., Miyahara, S., Zhang, X., Palo, S., Mlynczak, M., Mertens, C.J., & Hagan, M.E. (2006). Troposphere-thermosphere tidal coupling as measured by the SABER instrument on TIMED during July-September 2002. *J. Geophys. Res.*, Vol. 111, A10S06.

Gubbins, D., Jones, A.L., & Finlay, C.C. (2006). Fall in Earth's magnetic field is erratic. *Science*, Vol. 312, pp. 900-902.

Hagan, M.E., & Forbes, J.M. (2002). Migrating and nonmigrating diurnal tides in the middle and upper atmosphere excited by tropospheric latent heat release. *J. Geophys. Res.*, Vol. 107, No. D24, 4754.

Hagan, M.E., Maute, A., Roble, R.G., Richmond, A.D., Immel, T.J., & England, S.L. (2007). Connections between deep tropical clouds and the Earth's ionosphere. *Geophys. Res. Lett.*, Vol. 34, L20109.

Harris, M.J. (2001). *A new coupled middle atmosphere and thermosphere general circulation model: studies of dynamic, energetic and photochemical coupling in the middle and upper atmosphere*, PhD thesis, University College London, London, UK.

Häusler, K., Lühr, H., Rentz, S., & Köhler (2007). A statistical analysis of longitudinal dependences of upper thermospheric zonal winds at dip equator latitudes derived from CHAMP. *J. Atmos. Solar-Terr. Phys.*, Vol. 69, No. 12, pp. 1419-1430.

Haynes, P.H., Marks, C.J., McIntyre, M.E., Shepherd, T.G., & Shine, K.P. (1991). On the downward control of extratropical diabatic circulations by eddy-induced mean zonal forces. *J. Atmos. Sci.*, Vol. 48, No. 4, pp. 651-679.

Holt, J.M., & Zhang, S.R. (2008). Long-term temperature trends in the ionosphere above Millstone Hill. *Geophys. Res. Lett.*, Vol. 35, No. 5, L05813.

Hurst, D.F., Oltmans, S.J., Vömel, H., Rosenlof, K.H., Davis, S.M., Ray, E.A., Hall, E.G., & Jordan, A.F. (2011). Stratospheric water vapor trends over Boulder, Colorado: Analysis of the 30 year Boulder record. *J. Geophys. Res.*, Vol. 116, D02306.

Immel, T.J., Sagawa, E., England, S.L., Henderson, S.B., Hagan, M.E., Mende, S.B., Frey, H.U., Swenson, C.M., & Paxton, L.J. (2006). Control of equatorial ionospheric morphology by atmospheric tides. *Geophys. Res. Lett.*, Vol. 33, L15108.

Jarvis, M.J., Clilverd, M.A., & Ulich, Th. (2002). Methodological influences on F-region peak height trend analyses, *Phys. Chem. Earth,* Vol. 27, pp. 589-594.

Jarvis, M.J. (2009). Longitudinal variation in E- and F-region ionospheric trends. *J. Atmos. Solar-Terr. Phys.*, Vol. 71, 1415-1429.

Keating, G.M., Tolson, R.H., & Bradford, M.S. (2000). Evidence of long term global decline in the Earth's thermospheric densities apparently related to anthropogenic effects. *Geophys. Res. Lett.*, Vol. 27, No. 10, pp. 1523-1526.

Kivelson, M.G. & Russell, C.T. (Eds.) (1995). *Introduction to space physics*. Cambridge University Press, ISBN 0-521-45714-9, Cambridge, UK.

Laštovička, J. (2005). On the role of solar and geomagnetic activity in long-term trends in the atmosphere-ionosphere system. *J. Atmos. Solar Terr. Phys.*, Vol. 67, No. 1-2, pp. 83-92.

Laštovička, J., Akmaev, R.A., Beig, G., Bremer, J., & Emmert, J.T. (2006a). Global change in the upper atmosphere. *Science,* Vol. 314, No. 5803, pp. 1253-1254.

Laštovička, J., Mikhailov, A.V., Ulich, T., Bremer, J., Elias, A.G., Ortiz de Adler, N., Jara, V., Abaraca del Rio, R., Foppiano, A.J., Ovalle, E., & Danilov, A.D. (2006b). Long-term trends in foF2: A comparison of various methods. *J. Atmos. Solar-Terr. Phys.*, Vol. 68, pp. 1854-1870.

Lean, J.L., White, O.R., Livingstone, C., & Picone, J.M. (2001). Variability of a composite chromospheric irradiance index during the 11-year activity cycle and over longer time periods. *J. Geophys. Res.,* Vol. 106, No. A6, pp. 10645-10658.

Macmillan, S., & Droujinina, A. (2007). Long-term trends in geomagnetic daily variation. *Earth Planets Space*, Vol. 59, pp. 391-195.

Marcos, F.A., Wise, J.O., Kendra, M.J., Grossbard, N.J., & Bowman, B.R. (2005). Detection of a long-term decrease in thermospheric neutral density. *Geophys. Res. Lett.*, Vol. 32, L04103.

Pap, J.M., & Fox, P. (Eds.). (2004). *Solar variability and its effects on climate*, Geophysical Monograph 141, American Geophysical Union, ISBN 0-87590-406-8, USA.

Qian, L., Roble, R.G., Solomon, S.C., & Kane, T.J. (2006). Calculated and observed climate change in the thermosphere, and a prediction for solar cycle 24. *Geophys. Res. Lett.*, Vol. 33, L23705.

Qian, L., Burns, A.G., Solomon, S.C., & Roble, R.G. (2009). The effect of carbon dioxide cooling on trends in the F2-layer ionosphere. *J. Atmos. Solar-Terr. Phys.,* Vol. 71, pp. 1592-1601.

Qian, L., & Solomon, S.C. (2011). Thermospheric density: an overview of temporal and spatial variations, *Space Sci. Rev.*, in press, doi.: 10.1007/s11214-011-9810-z.

Qian, L., Laštovička, J., Roble, R.G., & Solomon, S.C. (2011). Progress in observations and simulations of global change in the upper atmosphere. *J. Geophys. Res.*, Vol. 116, A00H03.

Richmond, A.D., Ridley, E.C., & Roble, R.G. (1992). A thermosphere-ionosphere general circulation model with coupled electrodynamics. *Geophys. Res. Lett.*, Vol. 19, No. 6, pp. 601-604.

Rinsland, C.P., Chiou, L., Boone, C., Bernath, P., Mahieu, E., & Zander, R. (2009). Trend of lower stratospheric methane (CH_4) from atmospheric chemistry experiment (ACE) and atmospheric trace molecule spectroscopy (ATMOS) measurements, *J. Quant. Spectr. Rad. Transfer*, Vol. 110, pp. 1066-1071.

Rishbeth, H. (1990). A greenhouse effect in the ionosphere? *Plan. Space Sci.*, Vol. 38, No. 7, pp. 945-948.

Rishbeth, H. (1998). How the thermospheric circulation affects the ionospheric F2-layer. *J. Atmos. Solar-Terr. Phys.*, Vol. 60, 1385-1402.

Roble, R.G., Ridley, E.C., Richmond, A.D., Dickinson, R.E. (1988). A coupled thermosphere ionosphere general circulation model. *Geophys. Res. Lett.*, Vol. 15, No. 12, pp. 1325-1328.

Roble, R.G., & Dickinson, R.E. (1989). How will changes in carbon-dioxide and methane modify the mean structure of the mesosphere and thermosphere? *Geophys. Res. Lett.*, Vol. 16, No. 12, pp. 1441-1444.

Rosenlof, K.H., Oltmans, S.J., Kley, D., Russell III, J.M., Chiou, E.W., Chu, W.P., Johnson, D.G., Kelly, K.K., Michelsen, H.A., Nedoluha, G.E., Remsberg, E.E., Toon, G.C., & McCormick, M.P. (2001). Stratospheric water vapour increases over the past half-century. *Geophys. Res. Lett.*, Vol. 28, No. 7, pp. 1195-1198.

Sassi, F., Garcia, R.R., Marsh, D., & Koppel, K.W. (2010). The role of the middle atmosphere in simulations of the troposphere during northern hemisphere winter: differences between high- and low-top models. *J. Atmos. Sci.,* Vol. 67, No. 9, pp. 3048-3064.

Salby, M., Titova, E., & Deschamps, L. (2011). Rebound of Antarctic ozone. *Geophys. Res. Lett.*, Vol. 38, L09702.

Saunders, A., Lewis, H., & Swinerd, G. (2011). Further evidence of long-term thermospheric density change using a new method of satellite ballistic coefficient estimation. *J. Geophys. Res.*, in press, doi.: 10.1029/2010JAO16358.

Semenov, A.I. (1996). Temperature regime of the lower thermosphere from emission measurements during the last decades. *Geomagn. Aeron.*, Vol. 36, No. 5, pp. 90-97.

She, C.-Y., Krueger, D.A., Akmaev, R.A., Schmidt, H., Talaat, E., & Yee, S. (2009). Long-term variability in mesopause region temperatures over Fort Collins, Colorado (41°N, 105°W) based on lidar observations from 1990 through 2007.

Shimazaki, T. (1955). World-wide variations in the height of the maximum electron density of the ionospheric F2 layer. *J. Radio Res. Labs. Japan*, Vol. 2, pp. 85-97.

Solomon, S. (1999). Stratospheric ozone depletion: a review of concepts and history. *Rev. Geophys.*, Vol. 37, No. 3, pp. 275-316.

Stamper, R., Lockwood, M., Wild, M.N., & Clark, T.D.G. (1999). Solar causes of the long-term increase in geomagnetic activity. *J. Geophys. Res.*, Vol. 104, pp. 28325-28342.

Stolarski, R. & Frith, S.M. (2006). Search for evidence of trend slow-down in the long-term TOMS/SBUV total ozone data record: the importance of instrument drift uncertainty. *Atmos. Chem. Phys.*, Vol. 6, pp. 4057-4065.

Ulich, Th. (2000). *Solar variability and long-term trends in the ionosphere.* PhD thesis, Sodankylä Geophysical Observatory Publications, No. 87, Sodankylä, Finland.

Wang, W., Wiltberger, M., Burns, A.G., Solomon, S.C., Killeen, T.L., Maruyama, N., & Lyon, J.G. (2004). Initial results from the coupled magnetosphere-ionosphere-thermosphere model: thermosphere-ionosphere responses. *J. Atmos. Solar-Terr. Phys.*, Vol. 66, No. 15-16, pp. 1425-1441.

Wang, W.B., Lei, J.H., Burns, A.G., Wiltberger, M., Richmond, A.D., Solomon, S.C., Killeen, T.L., Talaat, E.R., & Anderson, D.N. (2008). Ionospheric electric field variations during a geomagnetic storm simulated by a coupled magnetosphere ionosphere thermosphere (CMIT) model, *Geophys. Res. Lett.*, Vol. 35, No. 18, L18105.

Wiltberger, M., Wang, W., Burns, A.G., Solomon, S.C., Lyon, J.G., & Goodrich, C.C. (2004). Initial results from the coupled magnetosphere ionosphere thermosphere model: magnetospheric and ionospheric responses. *J. Atmos. Solar-Terr. Phys.*, Vol. 66, No. 15-16, pp. 1411-1423.

Zhang, S.-R., Holt, J.M., & Kurdzo, J. (2011), Millstone Hill ISR observations of upper atmospheric long-term changes: Height dependency, *J. Geophys. Res.*, Vol. 116, A00H05.

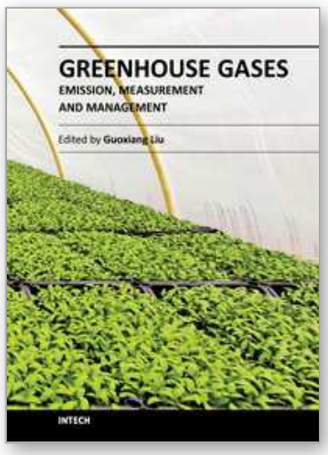

Greenhouse Gases - Emission, Measurement and Management
Edited by Dr Guoxiang Liu

ISBN 978-953-51-0323-3
Hard cover, 504 pages
Publisher InTech
Published online 14, March, 2012
Published in print edition March, 2012

Understanding greenhouse gas sources, emissions, measurements, and management is essential for capture, utilization, reduction, and storage of greenhouse gas, which plays a crucial role in issues such as global warming and climate change. Taking advantage of the authors' experience in greenhouse gases, this book discusses an overview of recently developed techniques, methods, and strategies: - A comprehensive source investigation of greenhouse gases that are emitted from hydrocarbon reservoirs, vehicle transportation, agricultural landscapes, farms, non-cattle confined buildings, and so on. - Recently developed detection and measurement techniques and methods such as photoacoustic spectroscopy, landfill-based carbon dioxide and methane measurement, and miniaturized mass spectrometer.

INTECH
open science | open minds

InTech Europe
University Campus STeP Ri
Slavka Krautzeka 83/A
51000 Rijeka, Croatia
Phone: +385 (51) 770 447
Fax: +385 (51) 686 166
www.intechopen.com

InTech China
Unit 405, Office Block, Hotel Equatorial Shanghai
No.65, Yan An Road (West), Shanghai, 200040, China
中国上海市延安西路65号上海国际贵都大饭店办公楼405单元
Phone: +86-21-62489820
Fax: +86-21-62489821

IntechOpen